DOI: 10.13009/EUCASS2019-736

On the UPMSat-2 Attitude, Control and Determination Subsystem's design

Elena Rodríguez-Rojo, Javier Cubas**, Elena Roibás-Millán*** and Santiago Pindado*****

Instituto Universitario de Microgravedad "Ignacio Da Riva" (IDR/UPM)
ETSI Aeronáutica y del Espacio, Universidad Politécnica de Madrid
Plaza del Cardenal Cisneros, 3
28040 Madrid, Spain

* *elena.rodriguez.rojo@upm.es*
***j.cubas@upm.es*
****santiago.pindado@upm.es*
*****elena.roibas@upm.es*

Abstract

In the present paper the work carried out in relation to the Attitude, Control and Determination Subsystem (ACDS) of the UPMSat-2 is summarized. This engineering project is integrated within the UPMSat-2 mission framework. This 50-kg satellite has been designed and manufactured by the Polytechnic University of Madrid (Universidad Politécnica de Madrid).

The development of this ACDS comprises the selection of the different parts, sensors (magnetometers) and actuators (magnetorquers), the design of the control law, the testing campaigns of the different subsystem's parts, and its verification. The magnetometers and magnetorquers were tested in the IDR/UPM Institute facilities at Montegancedo campus, in order to check its accuracy. Besides, the effect of their uncertainty levels on the satellite's stabilization process once its normal attitude has been perturbed, were studied.

The control law is based on B-dot, being thoroughly simulated by using Monte Carlo analysis. Finally, the last testing campaign, carried out during the final integration stages of the satellite is also summarized. The results obtained show a strong and reliable spacecraft control subsystem.

1. Introduction

The UPMSat-2 is a 50-kg satellite designed and manufactured by the Polytechnic University of Madrid (*Universidad Politécnica de Madrid, UPM*). Figure 1 shows a sketch of the satellite UPMSat-2 where its structure and components can be seen. Table 1 shows the otuline of the mission. The payloads of the satellite are a magnetometer by Bartington^{TM}, reaction wheel by SSBV^{TM}, thermal microswitch by Iberespacio^{TM}, on-board computer (E-BOX) by Tecnobit and solar sensors and thermal sensors systems developed by the UPM.

The project is framed within the Master's Degree in Space Systems (*Master Universitario en Sistemas Espaciales, MUSE*) and is designed to be both a technological demonstrator and a teaching tool for students. The learning occurs through the Project Base Learning (PBL) methodology [1]. The students, under the supervision of the teachers, participate both in the design of the subsystems, and in the validation tests of them. For this reason, the UPMSat-2 hardly has standardized elements. It does not use integrated commercial subsystems and does not use the CubeSat concept. Since 2012, thanks to this approach to the design and construction of the UPMSat-2, more than 20 student projects have been completed (Final Degree Projects / Final Master's Projects) in the degrees of Aeronautical Engineering and Space of the Polytechnic University of Madrid, having defended two doctoral theses, and another 3 are in progress.

DOI: 10.13009/EUCASS2019-736

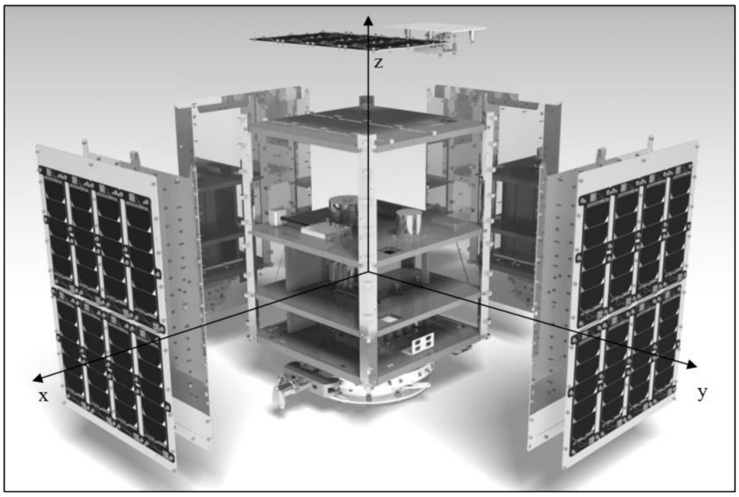

Figure 1: CAD drawing of the UPMSat-2 satellite.

Table 1: Outline of the UPMSat-2 Mission [2]

Mission Life	2 years
Orbit	Sun-synchronous: - 10:30 - Altitude: 500 km
Dimensions	0.5 m × 0.5 m × 0.6 m
Attitude Control	Magnetic: - SSBV24 magnetometers - ZARM Technik AG25 magnetorquers - Control law designed by IDR/UPM
Thermal Control	Passive
Power	Based on solar photovoltaic panels and batteries: - 5 body-mounted solar panels Selex Galileo - Li-ion battery designed by SAFT26 - Direct Energy Transfer (DET)
On board electronic box (E-BOX)	Based on FPGA (designed by Tecnobit S.L.27 and programmed by STRAST/UPM28). Includes: - On-board computer - Data handling - Power supply control - Power supply distribution
Communications	Link at 436 Mhz frequency

The structure of this article is as follows: In section 2 the ACDS subsystem of UPMSat-2 is described, including all the components. In Section 3 the attitude of UPMSat-2 is explained and the fundamentals of the control law are presented. In Section 4 a summary of main test performed to ADCS hardware is presented. Conclusions are in Section 5.

DOI: 10.13009/EUCASS2019-736

2. The ACDS subsystem

The attitude control of the UPMSat-2 has the following instruments:

Actuators
- Magnetorquer X
- Magnetorquer Y
- Magnetorquer Z
- Reaction wheel (experimental)

Sensors
- Magnetometer 1
- Magnetometer 2
- Magnetometer 3 (experimental)
- Solar panels (experimental)
- Photovoltaic cells (experimental)

In Figure 2 a diagram is presented with the distribution of some of the aforementioned elements in the Tray C of the satellite. Of the above elements, only the magnetorquers and magnetometers 1 and 2 are part of the nominal attitude control. The rest of the instruments will be used as part of the attitude control during the experimental phase. In the case of solar panels, the telemetry will be used in ground for a better understanding of the satellite orientation.

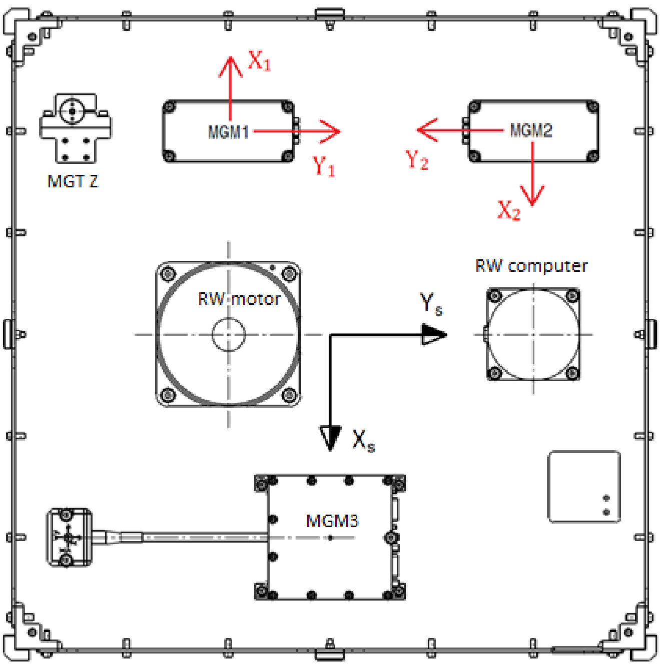

Figure 2: Diagram of UPMsat-2 Tray C.

2. The Control law

The law of attitude chosen to stabilize the satellite is represented in Figure 3. It has *Z* axis perpendicular to the orbit and a speed of rotation around it approximately constant and equal to 0.1 rad/s.

DOI: 10.13009/EUCASS2019-736

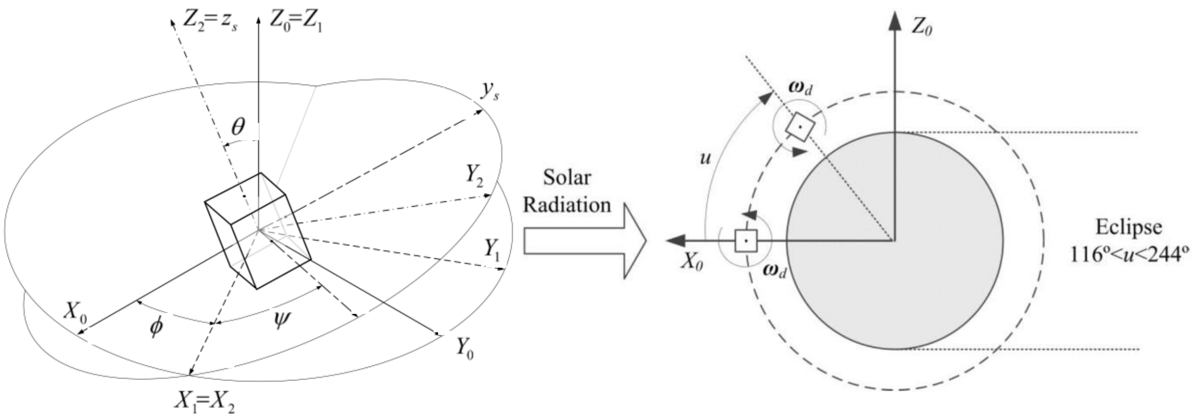

Figure 3: Left: UPMsat-2 axes. Right: diagram of UPMsat-2 attitude during the orbit

In the order of obtaining this attitude, a new control law based on a modification of the B-dot control law was designed [1]. The control algorithm of this law is based on the measurements of the magnetic field and its derivative. The algorithm calculates the magnetic moment that the magnetorquers must provide at each step of the attitude control. The control law is as follows:

$$m = -k_p \left({}^S\dot{B}_E + \omega_t \times {}^S B_E \right) \quad \textbf{(1)}$$

Where ${}^S B_E$ is the Earth's magnetic field in satellite body axes; ${}^S\dot{B}_E$ is its derivative; k_p is a constant of proportionality; and ω_t is the objective angular velocity.

One of the basic characteristics of this attitude control is that there is no need to determine the orientation. As can be seen in equation 1, the only element needed to calculate the control torque is the magnetic field in satellite body axes. Therefore the control algorithm is greatly simplified and the data processing needs are reduced.

Although the law of control does not change, the dynamics of the satellite goes through several successive phases as the attitude approaches the objective attitude (see Figure 4). The characteristics of these phases can be summarized as follows:

Detumbling phase:

- The satellite starts from an orientation and arbitrary angular velocities.
- The attitude control gradually reduces the angular velocities in *X* and *Y*-axis to zero, while correcting the angular velocity in *Z*-axis up to 0.1 rad/s.
- The orientation of the *Z*-axis with respect to the perpendicular to the orbit varies freely.

Orientation phase:

- Once the angular velocity has been corrected, the rotation axis (Z) tends to be oriented towards the perpendicular of the orbit (θ tends to zero).
- During the process the angular velocity remains stable, close to zero in *X* and *Y*-axis, and close to 0.1 rad/s in *Z*-axis.

Stable phase:

- The satellite keeps rotating around the X-axis with an angular velocity close to 0.1 rad/s.
- The rotation axis (*Z*) remains practically parallel to the normal to the orbit (θ close to zero).

DOI: 10.13009/EUCASS2019-736

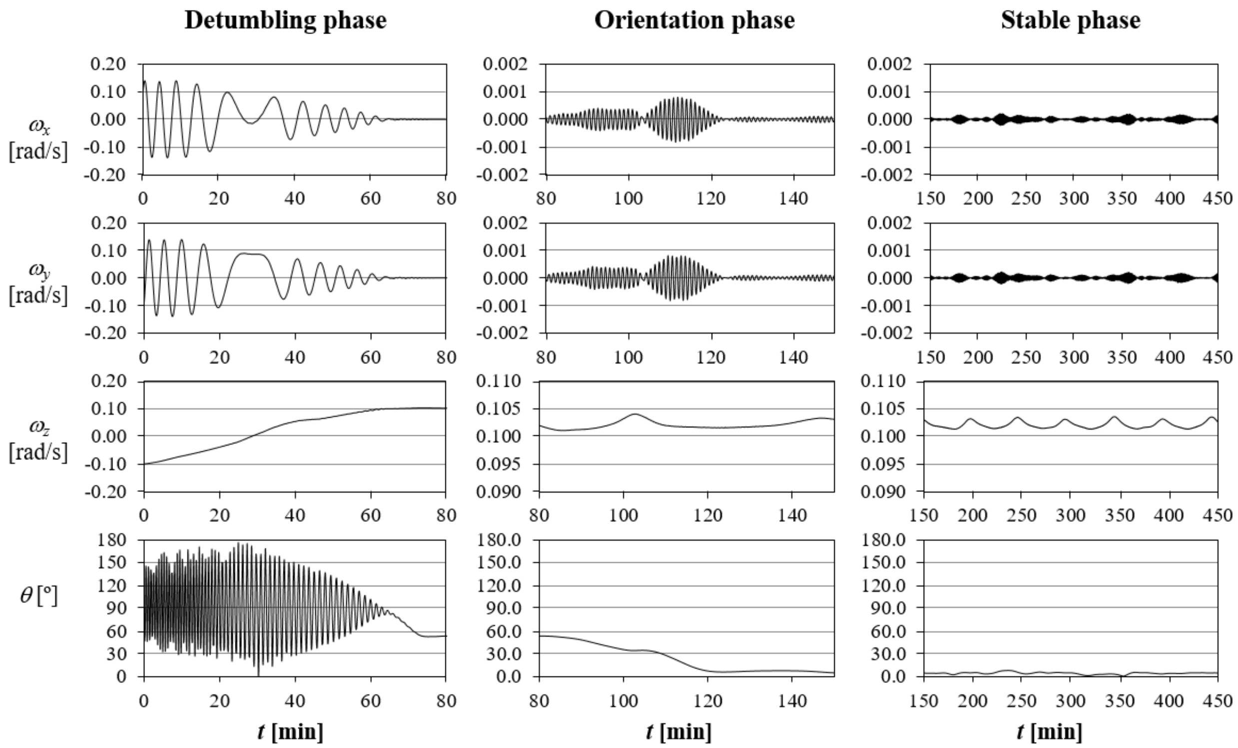

Figure 4: Example of performance of the UPMSat-2 angular velocity and orientation control.

Finally, we must add that the law of control only acts effectively on the angular velocity, and not on the orientation. The orientation of the satellite is guaranteed because, once the satellite is rotating, the equilibrium orientation has the rotation axis perpendicular to the orbit. This independence of the actuation gives robustness to the attitude control, ensuring that the axis of rotation will tend to be perpendicular to the orbit even the errors in the measurement of the magnetic field.

3. Test campaign

An important part of the UPMSat-2 project has been the tests and evaluations performed over the satellite. As an example we can mention the validation tests of the solar panels [4] or the battery [5]. In this section, a summary of some of the main milestones carried out during attitude control tests is presented. These tests included reception and operation tests. They were performed for sensors, actuators and data acquisition equipment, both separately and altogether. Despite the implementation of the control algorithm verification tests in the OBC can also be considered part of the ADCS tests, there are not the subject of this article. A summary of the latter can be found in [6].

3.1 Magnetometers

The UPMSat-2 has three magnetometers of two different manufacturers. Two of the magnetometers are from SSBV Space and Ground Systems Company, and the one remain is the Spacemag from Bartington Instruments Company. The magnetometers have been previously calibrated by the company that has provided them. And in the case of the SBVV ones a second most accurate calibration was done by the Imperial College of England. However, new tests and calibrations were performed, both for educational reasons and for ensuring that the calibration values provided were correct. The precautions proved reasonable since inconsistencies were detected in the pin numeration of the magnetometer connections.

All the magnetometers have three outputs, with three voltage measurements, which correspond to three perpendicular directions defined by the manufacturer. These voltage measurements are translated into electromagnetic field strength units thanks to the calibration algorithm. The input in this algorithm is the three measurements in magnetometer voltage, and the output is the magnetic field strength according to the three axes of the magnetometer.

DOI: 10.13009/EUCASS2019-736

In relation to the calibration algorithm, in a fluxgate magnetometer, like the ones considered in the present study, the relation between magnetic field measurements (in nano-Tesla) and the measurements in Volts given by the three axes, is as follows:

$$H_m = C^{-1}\left(B_m - b\right) \ . \quad \textbf{(2)}$$

where H_m is the magnetic field in magnetic units, C^{-1} is a symmetric matrix (expressed in nT V^{-1}), B_m is the magnetometer output in V and b is the offset vector (also expressed in V). The above equation is defined by means of a calibration process.

The errors in magnetometer measurements include biases, scale factors and misalignments. They can be classified into two main groups: environmental and instrumental errors. Considering all the aforementioned errors, the full measurement provided by the magnetometer can be expressed as:

$$B_m = SE\left(C^{si}H_m + b^{hi}\right) + b^{so} + v \ . \quad \textbf{(3)}$$

where S is the uncertainty in the scale factor, E the misalignment error, b^{so} the error in the calculation of the offset, C^{si} the soft iron perturbations (interactions with existing magnetic fields), b^{hi} the hard iron perturbations (constant magnetic fields) and v stands for a noise vector. All these errors can be grouped in the calibration parameters b^{*} and C^{*-1} :

$$H_m = C^{*-1}\left(B_m - b^{*}\right) \quad \textbf{(4)}$$

This expression allows, although the measurement provided by the magnetometer, B_m, is affected by the perturbations, to calculate a the magnetic field surrounding the magnetometer, H_m , discounting the disturbances. Several mathematical methods can be used to this purpose, being the most usual a version of a Least Square Method.

The basic calibration of a magnetometer is carried out in an environment in which the Earth's magnetic field is not disturbed by any other field. This entails performing the test in an environment free of elements that can generate or carry associated an electromagnetic field: electrical elements, current lines or ferromagnetic materials. Therefore, as a first approach to the performance of the magnetometer acceptance test, the verifications were done in open field, to avoid the presence of electronic devices. This first set of tests is described below. On the other hand, there have been trials dedicated to the recalibration of magnetometers, whose results are pending of publication.

To verify the correct calibration of the magnetometer, several types of measurements must be carried out:

- Measurement of the magnetic field according to defined directions, the intrinsic axes of the magnetometer, to determine the correct calibration of each of the axes.
- Measurement on the magnetic field module provided by the magnetometer for a group of space directions that sweep approximately one sphere.

As for the first part of the test, the procedure consisted of placing the magnetometer on a horizontal plane, with one of its axis vertically aligned and pointing towards the Earth, and the other one pointing towards the magnetic North Each set of measurements was carried out rotating the magnetometer in relation to the vertical axis and taking measurements in steps of 30 degrees [7]. The possible sources of errors (like are magnets, ferromagnetic materials and time-depending magnetic fields) can be found mostly in electronic devices and ferromagnetic materials (as tools, screws, bolts, power lines, sewage systems). Therefore, both outdoor and indoor tests were conducted, as to determine the importance of the disturbances of an indoor calibration process. Results from two of the tests carried out on two magnetometers, one of the SSBV magnetometers (FM008) and the Bartington magnetometer, are shown in Figure 5. In this figure the theoretical calculation of the projection of the Earth magnetic field H (the modulus value is provided by NOAA organization) on each one of the magnetometer axes is shown, and compared with different experimental results. A better accuracy can be appreciated from the outdoor testing, as had been expected.

The accuracy results of the tests were expressed in terms of the angle γ between the geomagnetic field, H, and the measured values, H_m, and the percentage difference between the modulus of both vectors. The margins of these magnitudes during the different tests are presented in Table 2.

DOI: 10.13009/EUCASS2019-736

Table 2: Accuracy errors of the UPMSat-2 magnetometers

Magnitude	**Indoor tests**	**Outdoor tests**
ΔH (%)	-5 to 5	-15 to 5
γ (deg)	2^o to 10^o	1^o to 4^o

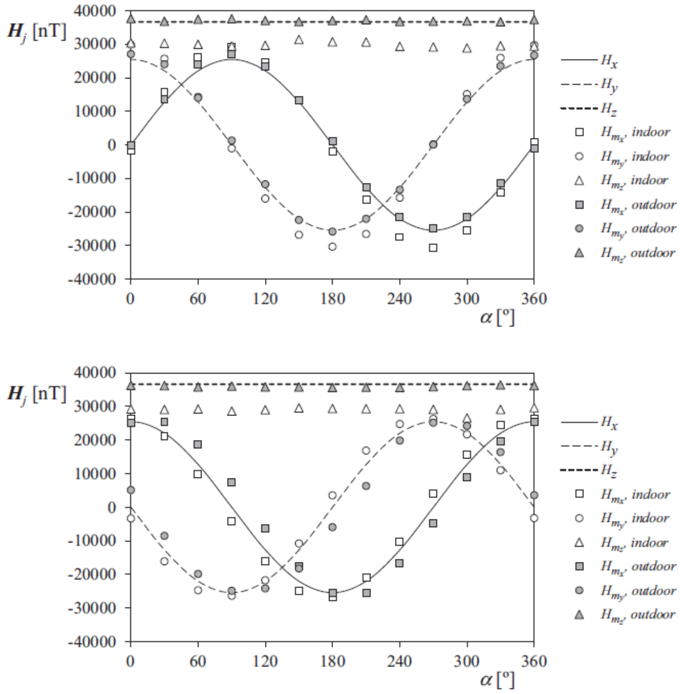

Figure 5: Components of the geomagnetic field H_m measured indoor and outdoor, in relation to the angular position of the magnetometer [7].

The results of the acceptance tests were considered valid given that, for the precision margins obtained, the simulations of the attitude control demonstrated a correct functioning of it. In reference [7] a more detailed analysis of how these errors can affect the operation of attitude control is also included.

Finally, in relation to the second measurements set, the one that is composed of scarcely spatial points, this method allows to determine statistics of the stability and accuracy of the magnetometers calibration.

3.2 Magnetorquers

The UPMSat-2 magnetorquers have been developed by Zarm Technik, an European company of the space sector. The units on-board, a total of three, consist of a set R/L (resistance coil, see Figure 6), which, subjected to a difference in voltage and, therefore, at a current flow, generates a magnetic moment. That is an electromagnet. The magnetic moment acts with the Earth's magnetic field generating a torque perpendicular to both.

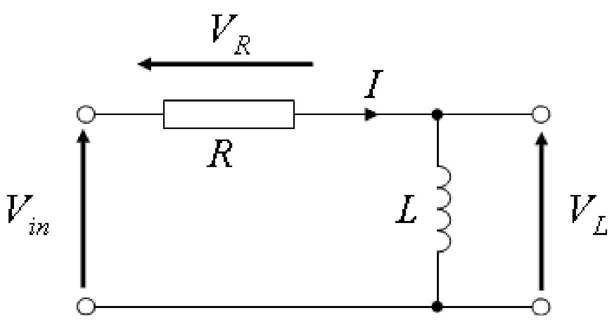

Figure 6: Scheme of the circuit of a magnetorquer.

DOI: 10.13009/EUCASS2019-736

The equation that describes the circuit of Figure 6 is:

$$V_{in} = I \cdot R + L \cdot \frac{dI}{dt} \quad . \tag{5}$$

Where V_{in} is the input voltage, I is the current, R is the resistance and L is the inductance. The magnetic moment generated by the coil can be expressed as:

$$m = I \cdot S \cdot n \; . \tag{6}$$

Where S is the section of the coil and n the number of turns of the coil. These two parameters are invariant. By expressing the intensity as a function of the magnetic moment, the equation (5) is:

$$\frac{dm}{dt} = \frac{S \cdot n}{L} V_{in} - \frac{R}{L} m = \frac{V_{in}}{a} - \frac{m}{b} \; . \tag{7}$$

And integrating the above equation:

$$m = \frac{b}{a} V_{in} \left(1 - e^{-\frac{t}{b}} \right) . \tag{8}$$

The variable b is the time constant of the circuit: the one for which when t takes its value, the magnetic moment is ($1-e^{-1}$) times the stationary value of m. And the stationary value is $b/a \cdot V_{in}$. The purpose of the acceptation tests were to define the transient and stationary behaviour of the magnetorquers. The transient through the calculation of the time constant b; and the stationary from the stationary value of the magnetic moment.

In Figure 7 one example of the curves that represent the variation of the magnetic moment generated by the magnetorquer obtained during the tests is presented. The magnetic moment is estimated through the current consumption. In Figure 8 it is possible to see the response of the magnetometer to the magnetorquer actuation. An electromagnet can be approximated to a magnetic dipole. The magnetic field generated by a magnetic dipole can be expressed as [9]:

$$\vec{B} = \frac{\mu_o}{4\pi} \frac{1}{\vec{R}^3} \left(3 \left(\vec{m} \frac{\vec{R}}{R} \right) \frac{\vec{R}}{R} - \vec{m} \right) . \tag{9}$$

Where μ_o is the magnetic permeability, constant value ($\mu_o = 4\pi \cdot 10^{-7}$ NA^{-2}) and $\vec{R}$ is the vector between the centre of the dipole and the position where $\vec{B}$ is calculated. Finally, $\vec{m}$ is the magnetic moment generated by the electromagnet. Equation (9) can be used to know the magnetic moment generated by the magnetorquers through the measurements of the magnetometers and the knowledge of the relative position.

DOI: 10.13009/EUCASS2019-736

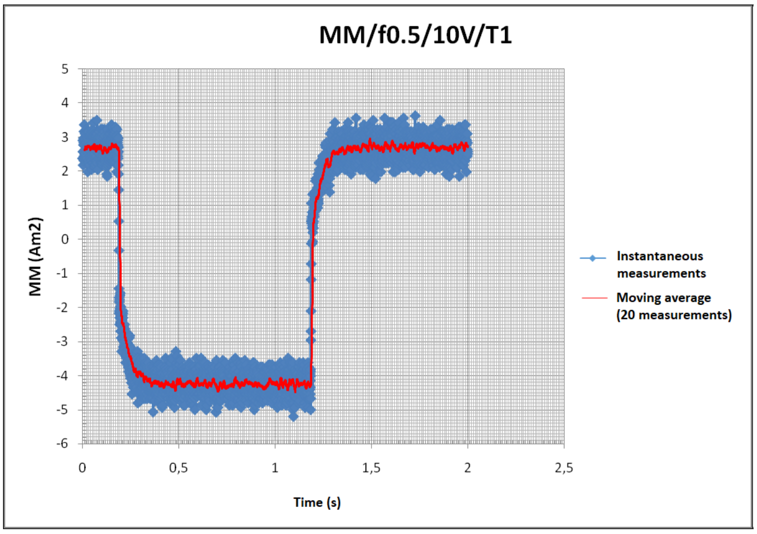

Figure 7: Test of magnetorquer actuation.

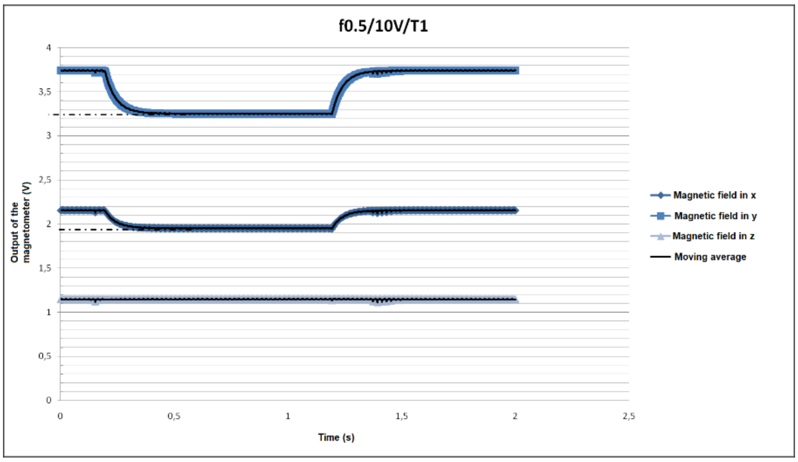

Figure 8: Magnetometer reaction to magnetorquer actuation.

The results of the tests determined that circuit constant was much lower than expected, 10 ms versus 51 ms specified by the manufacturer. This is equivalent to saying that the transient time of the circuit is smaller, experimentally, than expected by the specifications. This may be because the manufacturer's value is a conservative estimation or because the noise of the measurements is high and may have influenced the calculations. Nevertheless, the tests showed that the reaction times were as fast as required by the control.

Table 3: Comparison of experimental and manufacturer’s magnetic moment values

Test number	MM experimental	MM predicted by manufacturer
1	2.75	3
2	2.76	3
3	6.95	7
4	6.98	7
5	2.61	3
6	2.56	3
7	6.7	7
8	6.73	7

DOI: 10.13009/EUCASS2019-736

The magnetic moment obtained for the magnetorquers obtained through the tests and equation (9) are very similar to those provided by the manufacturer (see Table 3). The difference they present may be due to the difference in temperatures between the tests conducted by the manufacturer and the ones performed in the laboratory. We can conclude that the tests confirm the *I*/*V* ratio provided by the manufacturer it is sufficiently adjusted to reality and small variations will not substantially affect control.

3.3 Data acquisition

In addition to the sensors and actuators, another element that had to be calibrated was the data acquisition. The magnetometer measurements, which are in volts, have to be converted to digital data before they can be used by the control algorithm. This labour is performed by the Analogic-Digital Converter (ADC) integrated in the EBOX (electronic box) of the UPMSat-2. To perform these tests, a calibrated voltage source was used to obtain the relationship between the analog input and the digital output of the ADC. The indications of the manufacturer predict that the analog-digital conversion followed a linear law, within the saturation margins. However, the experimental tests showed that the linearity was not perfect (see Figure 9) and there were voltages for which the real conversion was quite far from what was expected (see Figure 10).

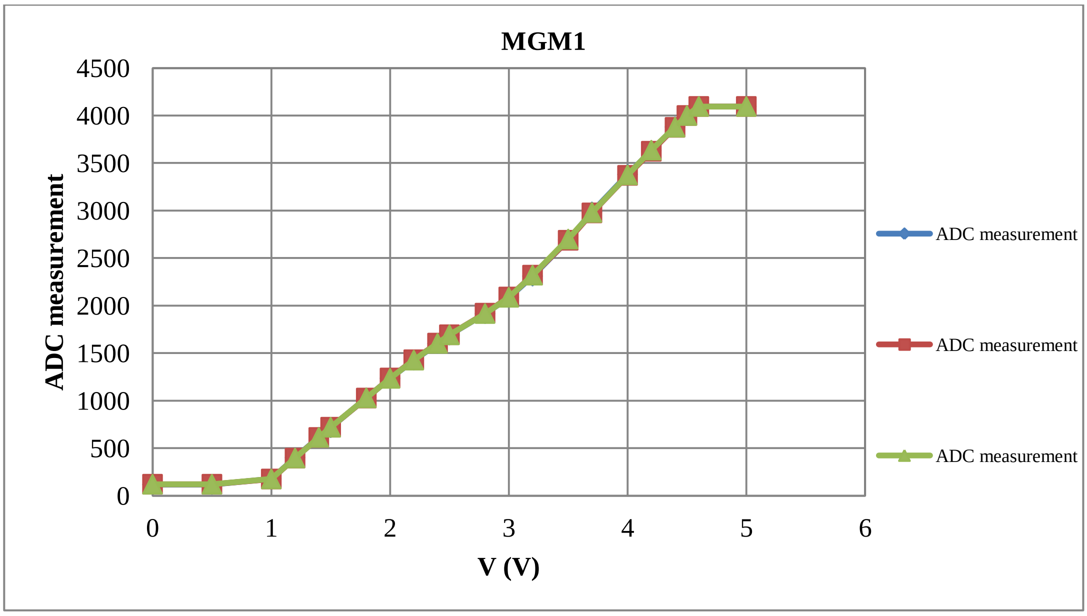

Figure 9: Characterization tests of the magnetometer 1 Analogic-Digital Converter.

The control algorithm of the UPMSat-2 was designed to interpret the measurements of the magnetometers provided by the ADC through a linear conversion to volts. So the poor performance of the ADC has meant a loss of precision in the attitude control performance. Fortunately, the simulations suggest that such loss of precision does not have an important effect on the performance of the control. But among the lessons learned for future missions is to include the characterization of the ADC as part of the control algorithm.

DOI: 10.13009/EUCASS2019-736

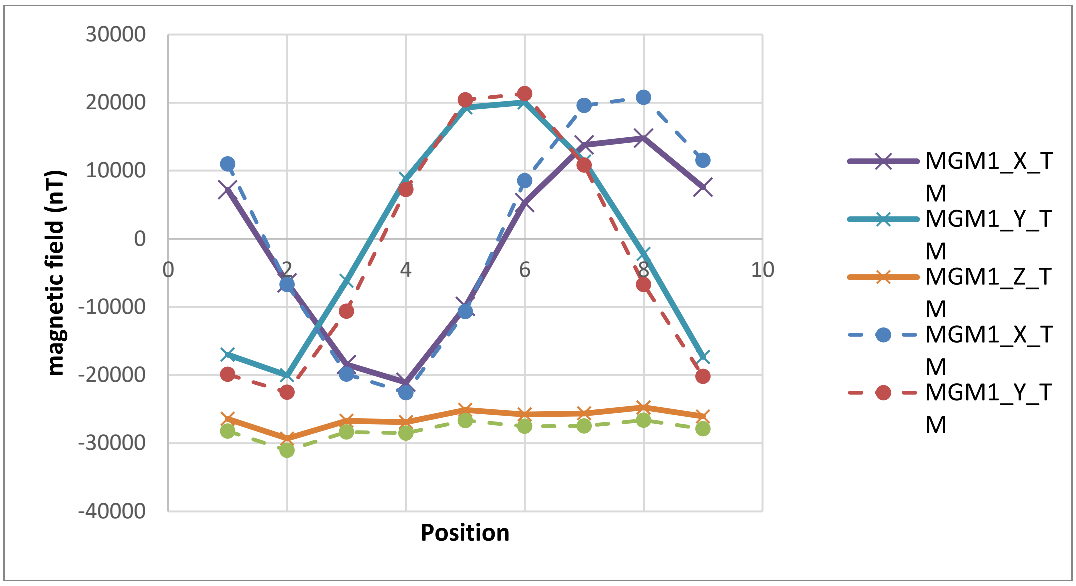

Figure 10: different interpretations of the measurements of the magnetometers.
Solid line: assuming linear conversion of the ADC. Dashed line: real non-linear ADC conversion.

3.4 Final tests

Once the satellite was assembled, it was necessary to make sure that the attitude control set worked correctly. In general, it is not enough to check the correct functioning of each of the elements separately from a system to ensure its overall functioning; the satellite has to been tested as an integrated system. In the case of the attitude control of the UPMSat-2, it was necessary to rule out the existence of errors in the hardware and software of data acquisition. Another element of uncertainty was the wiring of the harness. In addition, as can be seen in Figure 2, the mounting axes of the magnetometers do not coincide with those of the satellite. Therefore, in addition to the calibration, a change of axes had to be made to the magnetic field and it had to be proved that it had been done correctly.

The following simple tests were used to validate the operation of attitude control as a whole.

<u>Magnetometer initial test</u>

- The actuation of the magnetorquers is disconnected.
- The satellite is placed vertically with face X + pointing north.
- The measurements of magnetometers 1, 2 and 3 are collected and stored (every 0.2 sec).
    - Measurements of the ADC.
    - Data interpreted in nT.
- The procedure is repeated for the X-, Y +, Y- faces.
- The satellite is knocked down and the procedure is repeated on the faces Z + and Z-.

<u>Magnetorquer initial tests</u>

- The check routine is initiated.
    - The correct operation of the magnetorquers is verified including direction of magnetic moment through the measurements of the magnetometers.

<u>Static tests of attitude control.</u>

- Nominal attitude control operating mode is set.
- The satellite is placed vertically with face X + pointing north.
- The measurements of magnetometers 1, 2 and 3 are collected and stored (every 0.2 sec).
    - Measurements of the ADC.
    - Data interpreted in nT.
- At the same time, the on and off signals of the magnetorquers are collected and stored.

DOI: 10.13009/EUCASS2019-736

- The procedure for the X-, Y +, Y- faces is repeated.
- The satellite is knocked down and the procedure is repeated on the faces Z + and Z-.

<u>Dynamic tests of attitude control.</u>

- Nominal attitude control operating mode is set.
- The satellite is placed vertically with face X + pointing north.
- The satellite is rotated counter-clockwise (one revolution per minute) around the Z axis.
    - Measurements of the ADC.
    - Data interpreted in nT.
- Measures data in Tesla (intermediate value of attitude control)
- At the same time, the on and off signals of the magnetorquers are collected and stored.
- The satellite is knocked down and the procedure is repeated by turning around the X axis.

<u>Recalibration of magnetometers.</u>

- The actuation of the magnetorquers is disconnected.
- The satellite is placed vertically with face X + pointing north.
- The satellite is rotated counter-clockwise (one revolution per minute) around the Z axis.
- The measurements of magnetometers 1, 2 and 3 are collected and stored (every 0.2 sec).
    - Measurements of the ADC.
- The satellite is knocked down and the procedure is repeated by turning around the X axis.
- The satellite is rotated and the procedure is repeated by turning around the Y axis.

The initial tests were used to rule out faults in the wiring and in the acquisition of instrument data. As well as the correct conversion of digital measurements to units interpretable by the control law. The static test of attitude control was used to ensure that the attitude control correctly operated the magnetorquers.

In relation to the dynamic tests of attitude control, they were designed to ensure that the derivative of the magnetic field was correctly interpreted by the attitude control. However, it was found that the data acquisition was not fast enough to obtain interpretable results. Nevertheless, since this aspect had already been validated by hardware in the loop simulations, it was decided that the test could be omitted.

Finally, a recalibration of the magnetometers once assembled was considered. Although the magnetometers had already been calibrated in the acceptance tests, once assembled they can be exposed to environmental disturbances caused by the instruments in their surroundings or the satellite structure itself. In these tests, the environmental magnetic field (in conjunction with the satellite's own) was measured in a variety of positions to be able to use this data in the recalibration.

4. Conclusions

The present work summarizes the UPM-Sat2 ACDS design, integration and verification processes.

Related to the design, a derivate b-dot law is defined, which permits to fix a selected angular velocity and satellite orientation perpendicular to the orbital plane.

The ADCS sensors are two fluxgate magnetometers, which provide Volts measurements that are transformed in magnetic field measurements thanks to the calibration algorithm. This algorithm can be defined taking into account the possible environmental and instrumental disturbances.
Classical methods can be used to the algorithm determination, as the preference orientations methods. In addition to these classical swing methods, advanced mathematical methods can be defined, based in Least Squares derivatives. An implementation of this mathematical method is being developed as a future work in the UPM-Sat2 project scope.

In relation to the tests, acceptance tests were performed over the magnetometers and the magnetorquers. Apart from these aforementioned tests, the acquisition data system has been tested as well. The results of these tests are concluded to be compliance to the performance expected from the ADCS. All the testing procedure has been supported by design simulations of the ADCS satellite performance on-orbit. Robustness versus possible errors has been tested in different design simulations.

DOI: 10.13009/EUCASS2019-736

Finally, the satellite has been tested as an integrated system of the different subsystems. In particular, a recalibration of the sensors will be fulfilled using the measurements obtained during the mentioned tests. In a future, a dynamic recalibration will be considered. It will be calculated in ground segment and transmitted to the satellite as telemetry data.

DOI: 10.13009/EUCASS2019-736

References

[1] Pindado, S., Cubas, J., Roibás, E., Félix, M., and Palmer, S., "Project - based learning applied to spacecraft power systems : a long - term engineering and educational program at UPM University," *CEAS Space Journal*, Vol. 10, 2018, pp. 307–323. doi:10.1007/s12567-018-0200-1.

[2] Pindado, S., Roibas-millan, E., Garcia, A., Perez-grande, I., and Perez-alvarez, J., "The UPMSat-2 Satellite : An Academic Project within Aerospace Engineering Education," *Athens Institute for Education and Research ATINER ATINER's Conference Paper Series*, 2017, pp. 1–28.

[3] Cubas, J., Farrahi, A., and Pindado, S., "Magnetic Attitude Control for Satellites in Polar or Sun-Synchronous Orbits," *Journal of Guidance, Control, and Dynamics*, Vol. 38, 2015, pp. 1947–1958. doi:10.2514/1.G000751.

[4] Roibás-Millán, E., Alonso-Moragón, A., Jiménez-Mateos, A. G., and Pindado, S., "Testing solar panels for small-size satellites : the UPMSAT-2 mission," *Measurement Science and Technology*, Vol. 28, 2017, pp. 1–12.

[5] Porras-hermoso, Á., Pindado, S., and Cubas, J., "Lithium-ion battery performance modeling based on the energy discharge level," 2018.

[6] Garrido, J., Cubas, J., Zamorano, J., Cubas, J., Javier, A. De, Alonso, A., Alonso, A., and Puente, J. A. De, "The Design and Implementation of the UPMSAT-2 Attitude Control System," *IFAC-PapersOnLine*, Vol. 50, 2018, pp. 11245–11250. doi:10.1016/j.ifacol.2017.08.1607.

[7] Rodríguez-rojo, E., Pindado, S., Cubas, J., and Piqueras-carreño, J., "UPMSat-2 ACDS magnetic sensors test campaign," *Measurement*, 2018, p. doi:10.1016/j.measurement.2018.08.069.

[8] Wertz, J. R., *Spacecraft attitude determination and control*, Boston, MA: Springer Science & Business Media, 2012.